J|A|C|S
ARTICLES

Published on Web 04/02/2008

The Mechanism of the Rhodium(I)-Catalyzed [2 + 2 + 1] Carbocyclization Reaction of Dienes and CO: A Computational Study

William H. Pitcock Jr., Richard L. Lord, and Mu-Hyun Baik*

Department of Chemistry and School of Informatics, Indiana University, Bloomington, Indiana 47405

Received February 3, 2008; E-mail: mbaik@indiana.edu

Abstract: The rhodium(I) catalyzed [2 + 2 + 1] carbocyclization of tethered diene-enes to afford substituted hexahydropentalenones with high levels of diastereoselectivity was modeled using density functional theory. Previously, this transformation was observed to be facile, whereas the analogous bis-ene substrate could not be cyclized under any reasonable conditions. To establish a conceptual understanding of the carbocyclization mechanism and to identify the functional role of the diene fragment we analyzed the simulated reaction mechanisms using the two parent systems. We discovered a thus far unrecognized, but intuitively plausible, role of the CO ligand for controlling the electron density at the metal center, which affects the feasibility of oxidative addition and reductive elimination steps that are key components of the mechanism. Our calculations suggest that the diene moiety is unique and required because of its ability to undergo a $\eta^2 \rightarrow \eta^4$ reorganization allowing for the thermoneutral expulsion of one CO ligand, which in turn generates an electron-rich, coordinatively saturated Rh(I) center that can efficiently promote the oxidative addition with a low barrier. A number of functionalization strategies were considered explicitly to derive a rational plan for optimizing the catalysis and to expose the roles of the different components of the reactant−catalyst complex.

Introduction

The use of transition metals to promote otherwise difficult organic transformations is a powerful approach to constructing complex polycyclic systems efficiently. In particular, the exquisite control of stereochemistry displayed by transition metal catalysts and the ability to install multiple stereocenters simultaneously are two of the most attractive features of organometallic catalysis. While the breadth of the [$m + n + o$] carbocyclization variants is wide (e.g., [4 + 2], [5 + 2], [4 + 2 + 2], etc.),[1–18] the focus of this work is on the three component rhodium(I)-catalyzed [2 + 2 + 1] carbocyclization. One of the apparent requirements for the [2 + 2 + 1] carbocyclization is a "complex" π-system, either alkynes or allenes.[19–30] Building off the observation that diene-ynes reacted much faster than alkene-ynes, Wender postulated that the diene fragment could be used as a replacement for alkynes.[31–34] Indeed, the use of tethered diene-enes allowed for the convenient construction of cyclopentanones. Curiously, the presence of the diene fragment is critical, as analogous bis-ene substrates failed to react under

(1) Wender, P. A.; Jenkins, T. E. *J. Am. Chem. Soc.* **1989**, *111*, 6432–6434.
(2) Wender, P. A.; Jenkins, T. E.; Suzuki, S. *J. Am. Chem. Soc.* **1995**, *117*, 1843–1844.
(3) Jolly, R. S.; Luedtke, G.; Sheehan, D.; Livinghouse, T. *J. Am. Chem. Soc.* **1990**, *112*, 4965–4966.
(4) Gilbertson, S. R.; Hoge, G. S. *Tetrahedron Lett.* **1998**, *39*, 2075–2078.
(5) Gilbertson, S. R.; Hoge, G. S.; Genov, D. G. *J. Org. Chem.* **1998**, *63*, 10077–10080.
(6) Wender, P. A.; Takahashi, H.; Witulski, B. *J. Am. Chem. Soc.* **1995**, *117*, 4720–4721.
(7) Wender, P. A.; Sperandio, D. *J. Org. Chem.* **1998**, *63*, 4164–4165.
(8) Wender, P. A.; Glorius, F.; Husfeld, C. O.; Langkopf, E.; Love, J. A. *J. Am. Chem. Soc.* **1999**, *121*, 5348–5349.
(9) Wender, P. A.; Fuji, M.; Husfeld, C. O.; Love, J. A. *Org. Lett.* **1999**, *1*, 137–139.
(10) Trost, B. M.; Toste, F. D.; Shen, H. *J. Am. Chem. Soc.* **2000**, *122*, 2379–2380.
(11) Wender, P. A.; Husfeld, C. O.; Langkopf, E.; Love, J. A. *J. Am. Chem. Soc.* **1998**, *120*, 1940–1941.
(12) Wender, P. A.; Barzilay, C. M.; Dyckman, A. J. *J. Am. Chem. Soc.* **2001**, *123*, 179–180.
(13) Evans, P. A.; Robinson, J. E.; Baum, E. W.; Fazal, A. N. *J. Am. Chem. Soc.* **2002**, *124*, 8782–8783.
(14) Evans, P. A.; Robinson, J. E.; Baum, E. W.; Fazal, A. N. *J. Am. Chem. Soc.* **2003**, *125*, 14648–14648.
(15) Gilbertson, S. R.; DeBoef, B. *J. Am. Chem. Soc.* **2002**, *124*, 8784–8785.
(16) Evans, P. A.; Baum, E. W. *J. Am. Chem. Soc.* **2004**, *126*, 11150–11151.
(17) Evans, P. A.; Baum, E. W.; Fazal, A. N.; Pink, M. *Chem. Commun.* **2005**, 63–65.
(18) Baik, M. H.; Baum, E. W.; Burland, M. C.; Evans, P. A. *J. Am. Chem. Soc.* **2005**, *127*, 1602–1603.
(19) Evans, P. A.; Robinson, J. E. *J. Am. Chem. Soc.* **2001**, *123*, 4609–4610.
(20) Khand, I. U.; Knox, G. R.; Pauson, P. L.; Watts, W. E. *J. Chem. Soc., Chem. Commun.* **1971**, 36.
(21) Hanson, B. E. *Comments Inorg. Chem.* **2002**, *23*, 289–318.
(22) Brummond, K. M.; Kent, J. L. *Tetrahedron* **2000**, *56*, 3263–3283.
(23) Koga, Y.; Kobayashi, T.; Narasaka, K. *Chem. Lett.* **1998**, 249–250.
(24) Kobayashi, T.; Koga, Y.; Narasaka, K. *J. Organomet. Chem.* **2001**, *624*, 73–87.
(25) Jeong, N.; Lee, S.; Sung, B. K. *Organometallics* **1998**, *17*, 3642–3644.
(26) Jeong, N.; Sung, B. K.; Choi, Y. K. *J. Am. Chem. Soc.* **2000**, *122*, 6771–6772.
(27) Brummond, K. M.; Chen, H. F.; Fisher, K. D.; Kerekes, A. D.; Rickards, B.; Sill, P. C.; Geib, S. J. *Org. Lett.* **2002**, *4*, 1931–1934.

Scheme 1. Rhodium-Catalyzed [2 + 2 + 1] Carbocyclization of Diene-enes and Bis-enes

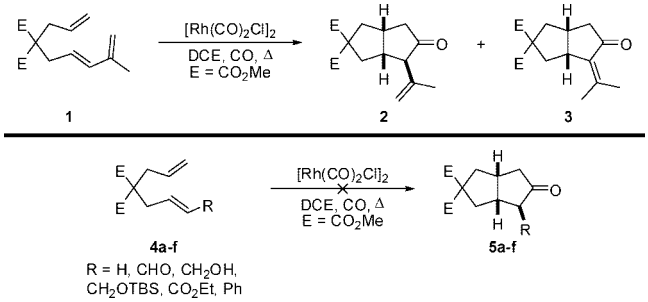

similar conditions (Scheme 1). Why the diene fragment is so important was not understood to date. Functionalized bis-ene analogues with coordinating heteroatoms or extended π-conjugation (**4a**−**f**) all failed to react, thus indicating that the role of the second double bond is not trivial. Simply providing an additional metal binding site or facilitating π-conjugation is clearly not enough to promote carbocyclization. We applied density functional theory (DFT)[35] to construct models of this reaction with the aim of identifying the function of the diene fragment during catalytic turnover and to highlight the deficiency of the bis-ene system. A systematic series of structural changes of the reactant−catalyst complex was constructed to highlight our conceptual understanding of the mechanism.

Computational Details

All calculations were carried out using the spin-restricted DFT formalism as implemented in the Jaguar 6.0[36] suite of ab initio quantum chemistry programs. Geometry optimizations were performed with the B3LYP[37–39] functional and the 6-31G** basis set with rhodium represented using the Los Alamos LACVP basis that includes relativistic effective core potentials.[40–42] The energies of the optimized structures were reevaluated by additional single-point calculations on each optimized geometry using Dunning's correlation-consistent triple-ζ basis set,[43] cc-pVTZ(-f), that includes the standard set of polarization functions. For Rh, we use a modified version of LACVP where the exponents have been decontracted to match the effective core potential with a triple-ζ quality basis. Vibrational frequency calculations based on analytical second derivatives at the B3LYP/6-31G** level of theory were carried out to derive the zero-point energy (ZPE) and entropy corrections at room temperature utilizing unscaled frequencies. Vibrational calculations were also used to confirm proper convergence to local minima or saddle points of the potential energy surface. Note that by entropy here we refer specifically to the vibrational/rotional/translational entropy of the solute(s); the entropy of the solvent is implicitly included in the dielectric continuum model. Solvation energies were evaluated by a self-consistent reaction field (SCRF)[44,45] approach based on accurate numerical solutions of the Poisson–Boltzmann equation.[46] In the results reported, solvation calculations were carried out at the optimized gas-phase geometry employing the dielectric constant of $\epsilon = 10.42$ (1,2-dichloroethane). As is the case for all continuum models, the solvation energies are subject to empirical parametrization of the atomic radii that are used to generate the solute surface. We employ the standard set of optimized radii in Jaguar for H (1.150 Å), C (1.900 Å), O (1.600 Å), Cl (1.974 Å), Br (2.095 Å), and Rh (1.464 Å). Partial atomic charges reported are based on atomic charges fit to the electrostatic potential.[47–49]

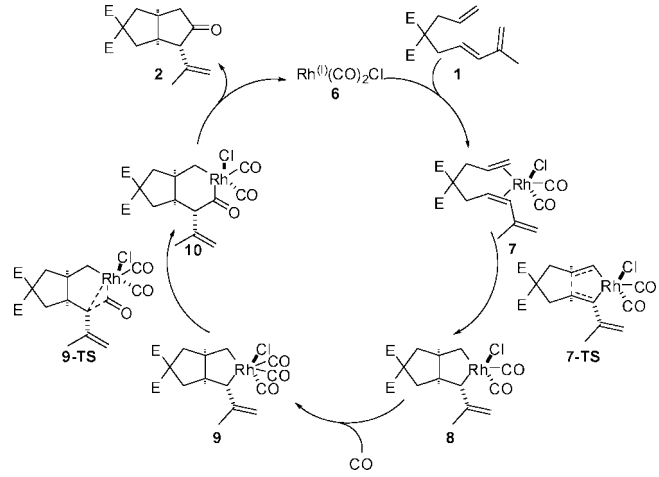

Figure 1. Mechanistic rationale for diene-ene [2 + 2 + 1] with $Rh(CO)_2Cl$ as catalyst.

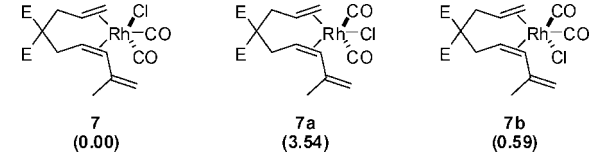

Figure 2. Possible $Rh(CO)_2Cl$ chlorine isomers during initial binding.

The energy components have been computed following the standard protocol. The free energy in solution phase G(sol) was calculated as follows:

$$G(\text{sol}) = G(\text{gas}) + G_{\text{solv}} \quad (1)$$

$$G(\text{gas}) = H(\text{gas}) + TS(\text{gas}) \quad (2)$$

$$H(\text{gas}) = E(\text{SCF}) + ZPE \quad (3)$$

where G(gas) is the free energy in gas phase, G_{solv} is the free energy of solvation as computed using the continuum solvation model, H(gas) is the enthalpy in the gas phase, T is the temperature (298.15

(28) Brummond, K. M.; Chen, H. F.; Mitasev, B.; Casarez, A. D. *Org. Lett.* **2004**, *6*, 2161–2163.
(29) Bayden, A. S.; Brummond, K. M.; Jordan, K. D. *Organometallics* **2006**, *25*, 5204–5206.
(30) Brummond, K. M.; Gao, D. *Org. Lett.* **2003**, *5*, 3491–3494.
(31) Wender, P. A.; Deschamps, N. M.; Gamber, G. G. *Angew. Chem., Int. Ed.* **2003**, *42*, 1853–1857.
(32) Wender, P. A.; Deschamps, N. M.; Williams, T. T. *Angew. Chem., Int. Ed.* **2004**, *43*, 3076–3079.
(33) Wender, P. A.; Croatt, M. P.; Deschamps, N. M. *Angew. Chem., Int. Ed.* **2006**, *45*, 2459–2462.
(34) Wender, P. A.; Croatt, M. P.; Deschamps, N. M. *J. Am. Chem. Soc.* **2004**, *126*, 5948–5949.
(35) Parr, R. G.; Yang, W. *Density Functional Theory of Atoms and Molecules*; Oxford University Press: New York, 1989.
(36) *Jaguar 6.0*; Schrödinger, Inc., Portland, Oregon, 2003.
(37) Becke, A. D. *Phys. Rev. A* **1988**, *38*, 3098–3100.
(38) Becke, A. D. *J. Chem. Phys.* **1993**, *98*, 5648–5652.
(39) Lee, C. T.; Yang, W. T.; Parr, R. G. *Phys. Rev. B* **1988**, *37*, 785–789.
(40) Hay, P. J.; Wadt, W. R. *J. Chem. Phys.* **1985**, *82*, 270–283.
(41) Hay, P. J.; Wadt, W. R. *J. Chem. Phys.* **1985**, *82*, 299–310.
(42) Wadt, W. R.; Hay, P. J. *J. Chem. Phys.* **1985**, *82*, 284–298.
(43) Dunning, T. H. *J. Chem. Phys.* **1989**, *90*, 1007–1023.
(44) Marten, B.; Kim, K.; Cortis, C.; Friesner, R. A.; Murphy, R. B.; Ringnalda, M. N.; Sitkoff, D.; Honig, B. *J. Phys. Chem.* **1996**, *100*, 11775–11788.
(45) Friesner, R. A.; Murphy, R. B.; Beachy, M. D.; Ringnalda, M. N.; Pollard, W. T.; Dunietz, B. D.; Cao, Y. X. *J. Phys. Chem. A* **1999**, *103*, 1913–1928.
(46) Edinger, S. R.; Cortis, C.; Shenkin, P. S.; Friesner, R. A. *J. Phys. Chem. B* **1997**, *101*, 1190–1197.
(47) Chirlian, L. E.; Francl, M. M. *J. Comput. Chem.* **1987**, *8*, 894–905.
(48) Woods, R. J.; Khalil, M.; Pell, W.; Moffat, S. H.; Smith, V. H. *J. Comput. Chem.* **1990**, *11*, 297–310.
(49) Breneman, C. M.; Wiberg, K. B. *J. Comput. Chem.* **1990**, *11*, 361–373.

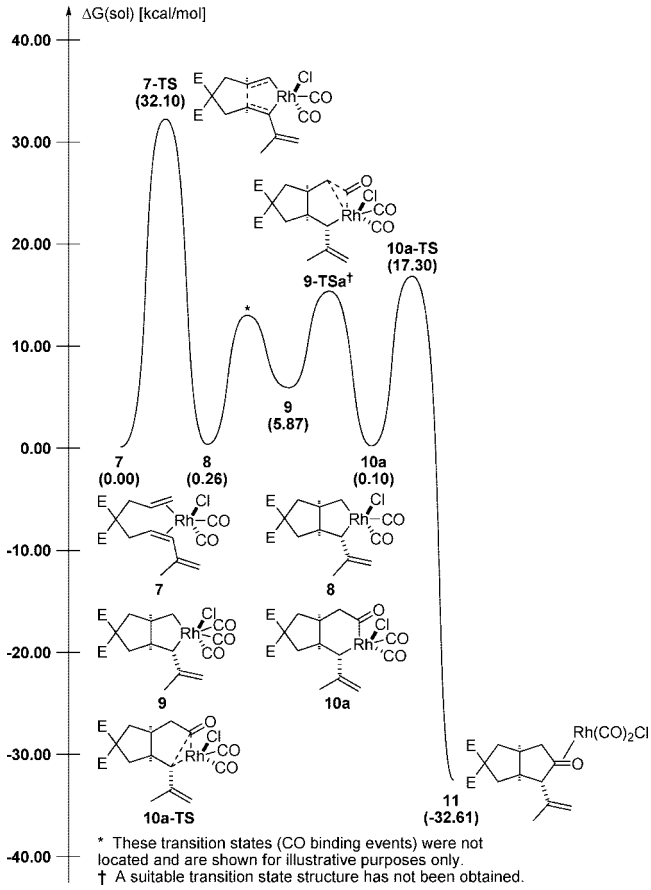

Figure 3. Reaction energy profile for diene-ene [2 + 2 + 1] using $Rh(CO)_2Cl$.

Scheme 2. Possible CO Insertion Regioisomeric Intermediates; Partial Charge *q* Is Indicated for **9**

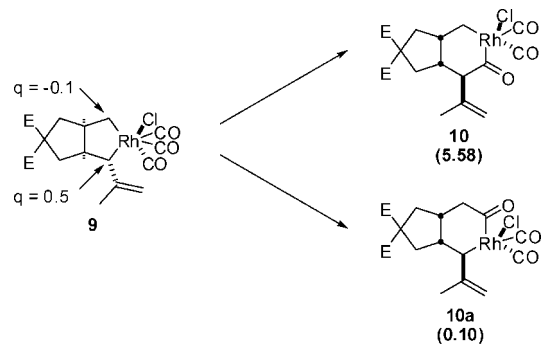

K), *S*(gas) is the entropy in the gas phase, *E*(SCF) is the self-consistent field energy, i.e., "raw" electronic energy as computed from the SCF procedure, and *ZPE* is the zero-point energy.

To locate transition states, the potential energy surface was first explored approximately, using the linear synchronous transit (LST) method,[50] followed by a quadratic synchronous transit (QST)[51] search using the LST transition state as an initial guess. In QST, the initial part of the transition-state search is restricted to a circular curve connecting the reactant, initial transition-state guess, and the product, followed by a search along the Hessian eigenvector that is most similar to the tangent of this curve. In certain cases (i.e., when structures were very similar), the QST-optimized transition states were refined by an unrestricted transition state search.

(50) Halgren, T. A.; Lipscomb, W. N. *Chem. Phys. Lett.* **1977**, *49*, 225–232.
(51) Peng, C. Y.; Schlegel, H. B. *Isr. J. Chem.* **1993**, *33*, 449–454.

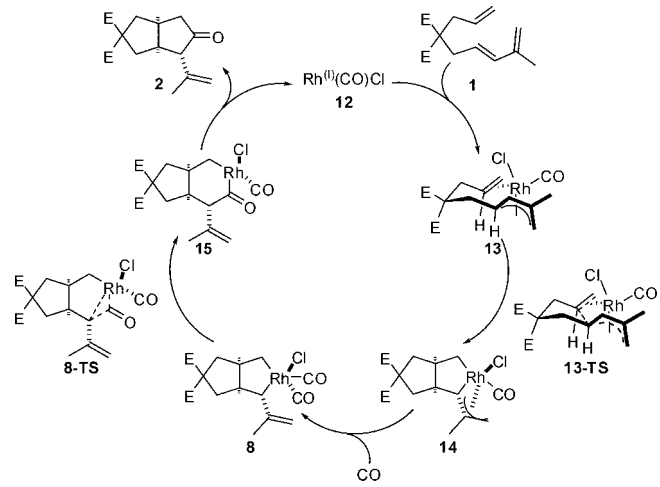

Figure 4. Mechanistic rationale for diene-ene [2 + 2 + 1] with Rh(CO)Cl as catalyst.

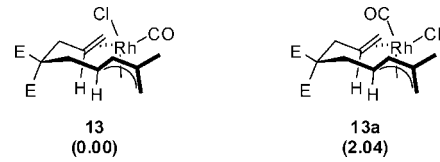

Figure 5. Possible Rh(CO)Cl chlorine isomers during initial binding.

Scheme 3. Possible CO Insertion Regioisomeric Intermediates; Partial Charge *q* Is Indicated for **8**

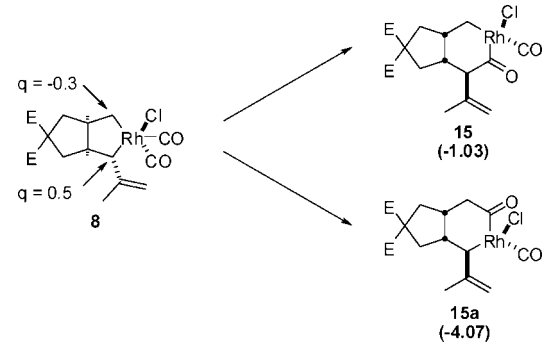

Results and Discussion

In many catalyst systems promoting organic transformations, the exact composition of the active catalyst is not known, which poses a difficult challenge to designing computer models of these reactions. A variety of possible structures must be explored carefully to identify a plausible catalyst complex that is most consistent with both experimental and theoretical considerations. For our model system, we used the reaction of diene-ene **1** with the most common catalyst found for this reaction, $[Rh(CO)_2Cl]_2$. Given the presence of CO in excess, we must also consider the presence of additional CO ligands at any point on the potential energy surface. The precatalyst $[Rh(CO)_2Cl]_2$ is commonly assumed to fragment in solution to give structurally identical 14-electron d^8 fragments, $Rh(CO)_2Cl$ (**6**), which bind the starting material in two distinct binding modes. The first involves binding **1** by utilizing only the alkene fragment and the proximal olefin of the diene to yield an 18-electron species (**7**, Figure 1).

After forming **7**, the complex undergoes oxidative addition via **7-TS** to form **8**, in which the three contiguous stereocenters

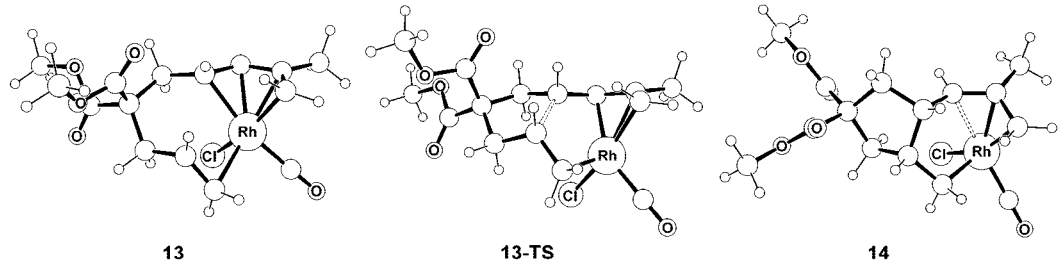

Figure 6. Computed structures for diene-ene binding, oxidative addition, and metallacyclopentane.

are simultaneously set. This results in a Rh(III), 16-electron adduct. Since the reaction is carried out under 1 atm of CO pressure, subsequent binding of an additional CO ligand to form the 18-electron complex **9** is feasible. This pseudo-octahedral complex now has the appropriate geometry and proximity to allow for facile CO insertion traversing **9-TS** to form the rhodacycle **10**, which can undergo reductive elimination to form the desired product **2** and regenerate the catalytic species **6**. One immediate question that arises is that of catalyst configuration. While one particular orientation is shown (**7**, Figure 1), it is possible to have two alternate isomers (Figure 2). Our studies suggest that the chloride ligand prefers the axial position *trans* to the pendant olefin by 3.5 kcal/mol over **7a** and 0.60 kcal/mol over **7b**.

The computed structures are distorted trigonal-bipyramidal and feature a slightly stronger binding to the isolated olefin as opposed to the proximal olefin of the diene. Another regiochemical issue to consider involves the direction of CO insertion. The CO ligand may either insert into the methine− or the methylene−rhodium bond to afford **10** and **10a**, respectively (Scheme 2). While this detail has no effect on the overall outcome of the reaction, it is *a priori* not clear how these two possible pathways will affect the reaction mechanism and must therefore be considered explicitly. Our calculations show that metallacyclohexanone **10a** is thermodynamically favored over **10** by 5.5 kcal/mol in solution-phase free energy. While initial arguments for this preference could be based on sterics, a more fundamental reason exists for this energetic advantage. The computed partial atomic charges[47–49] on the methylene and methine carbons are −0.1 and 0.5, respectively, indicating that the methylene carbon is more nucleophilic than the methine carbon. This charge polarization difference reflects of course on the stronger electron-withdrawing ability of the sp^2 carbons in the olefinic unit assisted by the resonance stabilization of the additional charge compared to a simple hydrogen fragment.

The complete reaction energy profile for the mechanism outlined above is illustrated in Figure 3. Oxidative addition is rate determining with a prohibitively high barrier of 32.1 kcal/mol, which would translate to a very slow reaction even at elevated temperatures. The remaining steps of the reaction mechanism are reasonable with low barriers connecting each of the intermediates. While a plausible transition state could not be obtained for the migratory insertion of CO despite intensive efforts, we do not expect the barrier to be high enough to give this step any physical meaning. Ziegler and co-workers demonstrated that migratory insertion of CO into Rh−alkyl bonds is relatively facile in methanol carbonylation, as compared to Ir where insertion is rate determining.[52] Previous studies on

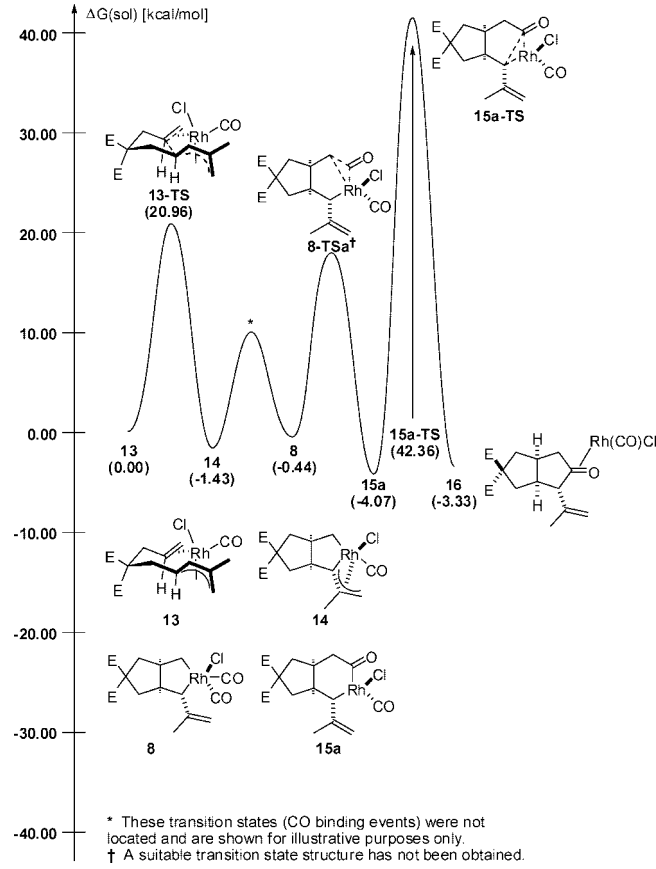

Figure 7. Reaction energy profile for diene-ene [2 + 2 + 1] using Rh(CO)Cl.

related systems also indicated that the oxidative addition is typically rate determining in Pauson−Khand [2 + 2 + 1] carbocyclizations.[53] The final step of the reaction, the reductive elimination to complete the carbocyclization, is associated with transition state **10a-TS** at a relative energy of 17.3 kcal/mol.

Although **7** is a plausible starting point for the carbocyclization, it is also possible that the diene fragment prefers to bind in an η^4 fashion instead of the η^2 binding mode shown in Figure 1. In this case, the 12-electron fragment Rh(CO)Cl serves as the catalytically competent species giving rise to a reaction pathway shown in Figure 4. **12** is unlikely to exist, however, as CO loss from **6** is unfavorable by 44.8 kcal/mol. Analogous to the mechanism discussed above, initial binding affords adduct **13** that undergoes oxidative addition through transition state **13-TS** to give metallacycle **14**. Addition of a CO ligand gives intermediate **8**, followed by CO insertion giving access to the

(52) Cheong, M.; Schmid, R.; Ziegler, T. *Organometallics* **2000**, *19*, 1973–1982.

(53) Wang, H.; Sawyer, J. R.; Evans, P. A.; Baik, M. H. *Angew. Chem., Int. Ed.* **2008**, *47*, 342–345.

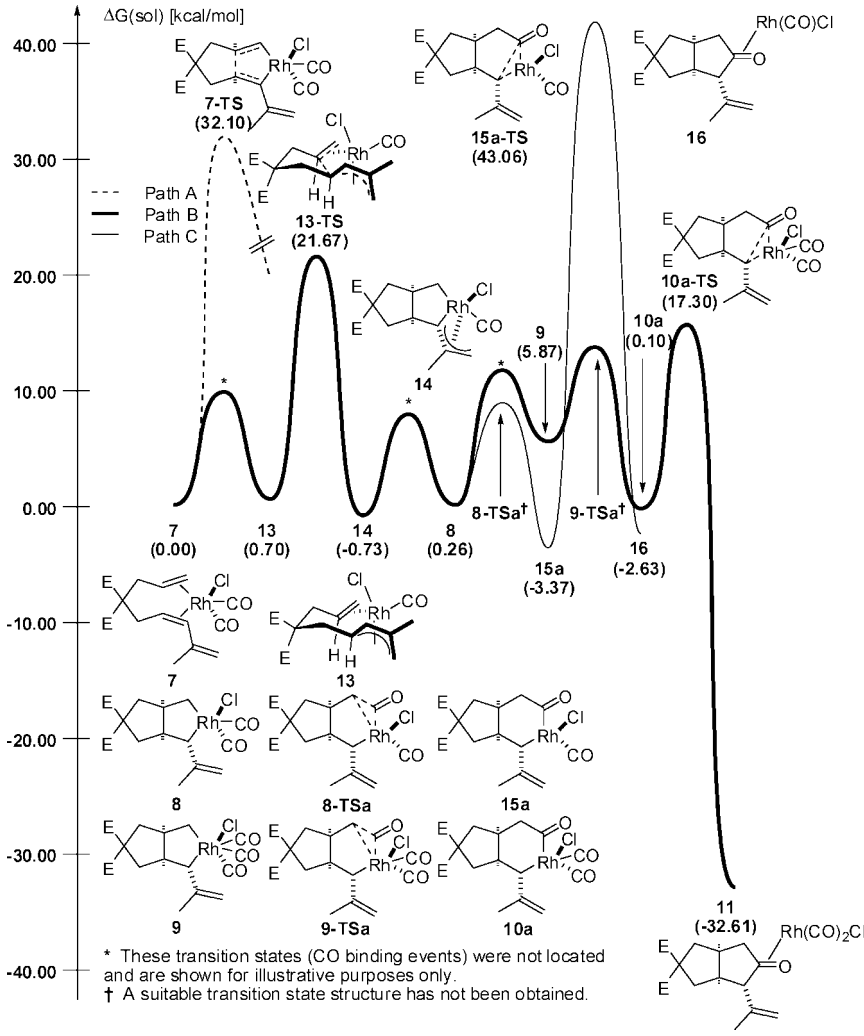

Figure 8. Combined reaction energy profile for diene-ene [2 + 2 + 1].

metallacyclohexanone **15**, which can reductively eliminate product **2** regenerating the catalyst **12**. As was the case with $Rh(CO)_2Cl$, it is possible for catalyst **12** to be bound to the diene-ene in one of two orientations (Figure 5). Our calculations indicate that isomer **13** is energetically preferred by ~2 kcal/mol over **13a**. For understanding the role of the diene fragment, it is crucial to recognize that binding the diene fragment in an η^4 fashion to the metal center gives rise to a three-legged piano stool type of coordination geometry. This structural feature is maintained throughout the oxidative addition, and even in metallacycle **14** where the metal center is in a slipped σ-allyl environment, as illustrated in Figure 6. This system also allows for the formation of regioisomeric intermediates (Scheme 3). For this pathway, CO insertion into the methylene−rhodium bond to form **15a** is favored over **15** by 3.1 kcal/mol and the partial charges indicate again that the methylene carbon is significantly more nucleophilic than the methine carbon.

The full reaction energy profile for the carbocyclization of diene-ene **1** using **12** as the catalytically competent metal complex is shown in Figure 7. We label this profile as the "low CO pressure case," as we expect the low-coordination Rh-complex to exhibit increased population under reduced CO pressure conditions, whereas $Rh(CO)_2Cl$ discussed above is expected to be the dominant composition of the catalyst under high CO-pressure conditions. The oxidative addition step associated with the transition state **13-TS** is easily accessible with a free energy barrier of 21.0 kcal/mol to give intermediate **14** that is 1.4 kcal/mol lower in energy than the reactant complex. CO binding to **14** to form **8** should be facile, albeit slightly uphill. While the CO insertion transition state **8-TSa** could not be located, it can be estimated in a similar fashion as for the reaction of $Rh(CO)_2Cl$. Interestingly, the rate-determining step for this mechanistic route is not the oxidative addition, unlike what we found for the "high CO pressure" manifold described above. With a free energy of activation of 42.4 kcal/mol associated with the transition state **15a-TS**, the reductive elimination has become the rate-determining step. A kinetic barrier of this magnitude cannot be overcome under realistic conditions.

The two slightly different reaction pathways discussed above illustrate an interesting mechanistic scenario. In the high CO pressure case, the CO insertion and reductive elimination are highly accessible with low barriers, but the initial oxidative addition is difficult to complete. In contrast, the low CO pressure case gives kinetically facile oxidative addition, but affords intermediates that are unable to complete the reaction due to high barriers for the reductive elimination step. The two pathways considered above contain the common intermediate **8**, which can serve as a lynchpin to combine the two mechanistic scenarios into one reaction energy profile, shown in Figure 8. Initial complexation leads to **7**, followed by loss of a CO molecule to give the η^4-complex **13**. Interestingly, this is a

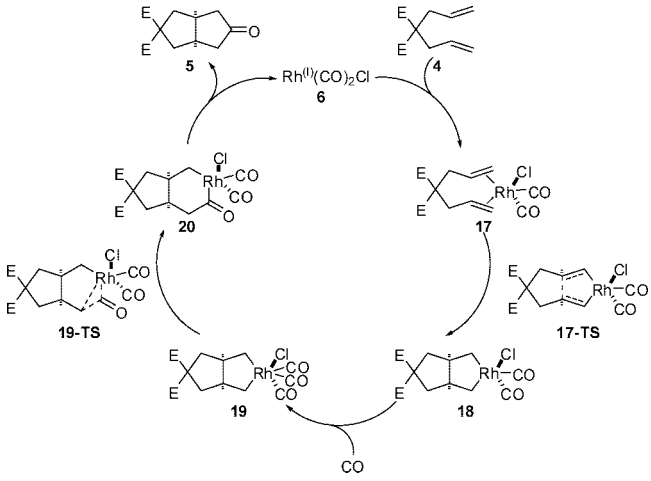

Figure 9. Mechanistic rationale for bis-ene [2 + 2 + 1] with $Rh(CO)_2Cl$ as catalyst.

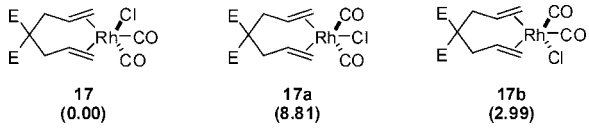

Figure 10. $Rh(CO)_2Cl$ positional isomers for bis-ene binding.

Table 1. Energy Components for the Intramolecular Binding of the Diene vs the Intermolecular Binding of CO in kcal/mol

step	ΔH(gas)	$-T\Delta S$(gas)	ΔG(gas)	ΔG_{solv}	ΔG(sol)
7 → 7-TS	34.18	1.14	35.32	−3.22	32.10
7 → 13	12.40	−8.73	3.67	−2.97	0.70
13 → 13-TS	20.82	−13.15	21.75	−0.79	20.96

thermoneutral process, suggesting that the η^4-binding compensates perfectly for the loss of CO. Note that this transformation should be entropically favored by approximately 10 kcal/mol at room temperature due to the release of translational entropy of CO. Since the entropy change for the intramolecular Rh-η^2 → Rh-η^4 rearrangement is expected to be significantly lower, the binding enthalpy of the diene does not have to fully compensate for the loss of Rh−CO bond energy. The computed energy components are shown in Table 1 and confirm our intuitive estimates. The **7 → 13** transformation, which encompasses the expulsion of CO and rearrangement of the diene fragment, is enthalpically (ΔH) uphill by 12.4 kcal/mol, reflecting on the fact that the Rh−CO bond is stronger than the new Rh−π bond formed. However, the release of CO is entropically favored, and our calculations estimate the energy gain associated with this process to be 8.7 kcal/mol. Differential solvation energy contributes 3.0 kcal/mol in favor of **13** to make this transformation overall thermoneutral. These energy components are important and will become highly relevant for understanding the role of the diene, as will be discussed below. The thermoneutrality suggests that a rapid pre-equilibrium may be established between the two different Rh-complexes in the presence of excess CO. The oxidative addition is best accomplished by following path B with an activation energy of 21.7 kcal/mol to form the slipped σ-allyl rhodacycle **14** with a solution-phase free energy of −0.7 kcal/mol. Binding of another CO molecule leads to the common intermediate **8**, where pathway bifurcation is encountered again. If path C is followed, the system will undergo CO insertion associated with the

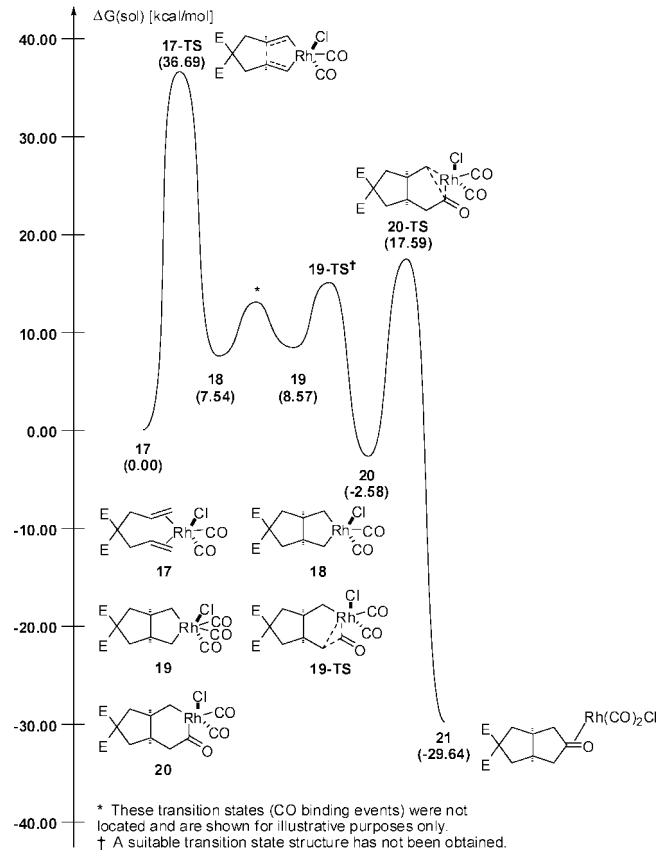

Figure 11. Reaction energy profile for bis-ene [2 + 2 + 1] using $Rh(CO)_2Cl$.

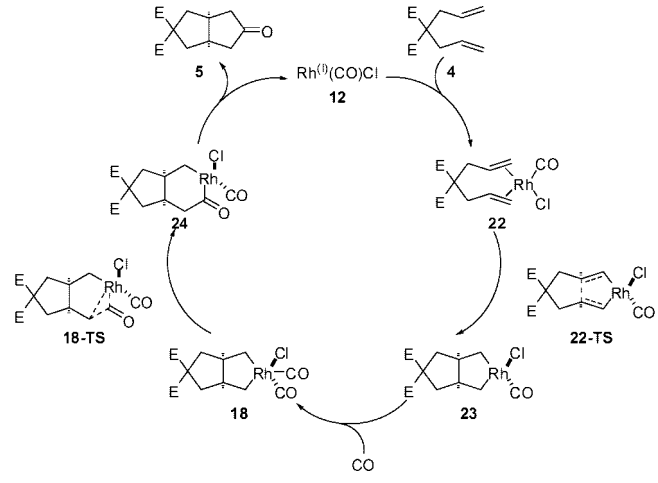

Figure 12. Mechanistic rationale for bis-ene [2 + 2 + 1] with Rh(CO)Cl as catalyst.

transition state **8-TSa** to form rhodacyclohexanone **15a**, where another bifurcation is encountered. The unproductive reductive elimination barrier via **15a-TS** prohibits conversion to the desired product along path C, however, **15a** could also directly bind CO to form **10a** on path B. Alternatively, if path B is followed from common intermediate **8** then CO binding leads to rhodacyclopentane **9** which followed by migratory insertion also leads to **10a.** Both post rate determining pathways to **10a** are likely operable and reductive elimination through this intermediate leads to the product-catalyst adduct **11**. Oxidative addition is rate determining with a barrier of 21.7 kcal/mol in this combined final mechanism, suggesting that the carbocy-

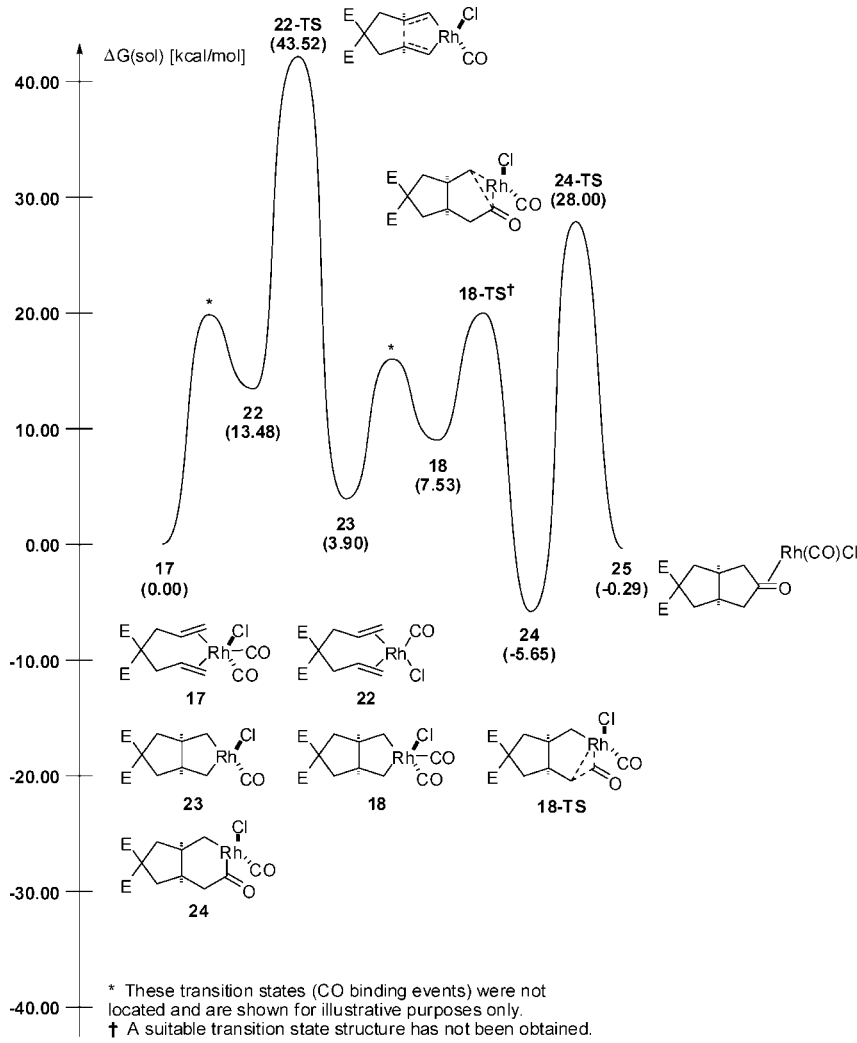

Figure 13. Reaction energy profile for bis-ene [2 + 2 + 1] using Rh(CO)Cl.

Table 2. Energy Component for the Binding of Various π-Bases in the Bis-ene System in kcal/mol

step	ΔH(gas)	$T\Delta S$(gas)	ΔG(gas)	ΔG_{solv}	ΔG(sol)
17 → **22**	27.94	−10.83	17.10	−3.62	13.48
22 → **26**	−5.61	11.22	5.61	3.58	9.19
26 → **26-TS**	31.53	2.34	33.88	−3.38	30.50
22 → **27**	−2.55	9.23	6.68	4.47	11.15
26 → **27-TS**	29.21	2.69	31.91	−0.40	31.51
22 → **28**	−3.29	13.32	10.02	4.61	14.63
26 → **28-TS**	29.55	1.08	30.63	−4.16	26.47
22 → **29**	0.44	10.70	11.14	5.23	16.37
26 → **29-TS**	26.69	3.36	30.05	−5.22	24.83

clization of **1** should be a facile process, in good agreement with experimental observations.[34]

The different reactivity as a function of the number of CO ligands coordinated to the Rh-center is fairly easy to understand. For the oxidative addition it is desirable for the metal to be electron rich. In **7** the π-withdrawing nature of the CO ligand reduces the electron density at the rhodium center, making the oxidative addition more difficult. CO loss and the subsequent η^4 binding of the diene lead to a much more electron-rich metal center, which facilitates the oxidative addition. Analogously, reductive elimination prefers an electron-poor metal center and the π-acidity of the CO ligand can be used again to control the electron density at the metal center. Intermediate **15a** with only one CO ligand is less effective in promoting reductive elimination than intermediate **10a**, which is formed by coordinating an additional CO. Our calculations also suggest a potential functional role for the diene moiety. The rate-determining step is the oxidative addition, as discussed above. The coordination of the electron-rich π-component after removal of the CO ligand from the initial reactant complex **7** helps to further increase the electron density of the metal center, thus, promoting oxidative addition. To better understand this synergistic interplay between the CO and diene ligand, we examined the simple bis-ene substrate **4** that cyclizes to afford **5**, as summarized in Figure 9.

Analogous to the mechanism discussed above, initial adduct **17** can undergo oxidative addition traversing the transition state **17-TS** to afford the metallacyclopentane **18**. CO binding followed by insertion affords metallacyclohexanone **20**, which can reductively eliminate to give **4** and regenerate the catalyst **6**. Again, we observe an energetic preference for the chloride ligand being in the axial position disposed *trans* to the olefinic methine protons by 8.8 kcal/mol over **17a** and 3.0 kcal/mol over **17b** (Figure 10). Unlike the diene-ene system, CO insertion isomers need not be considered in the bis-ene system as the reactant **4** is symmetrical.

The reaction energy profile shown in Figure 11 suggests that the reaction will not occur under realistic conditions. The

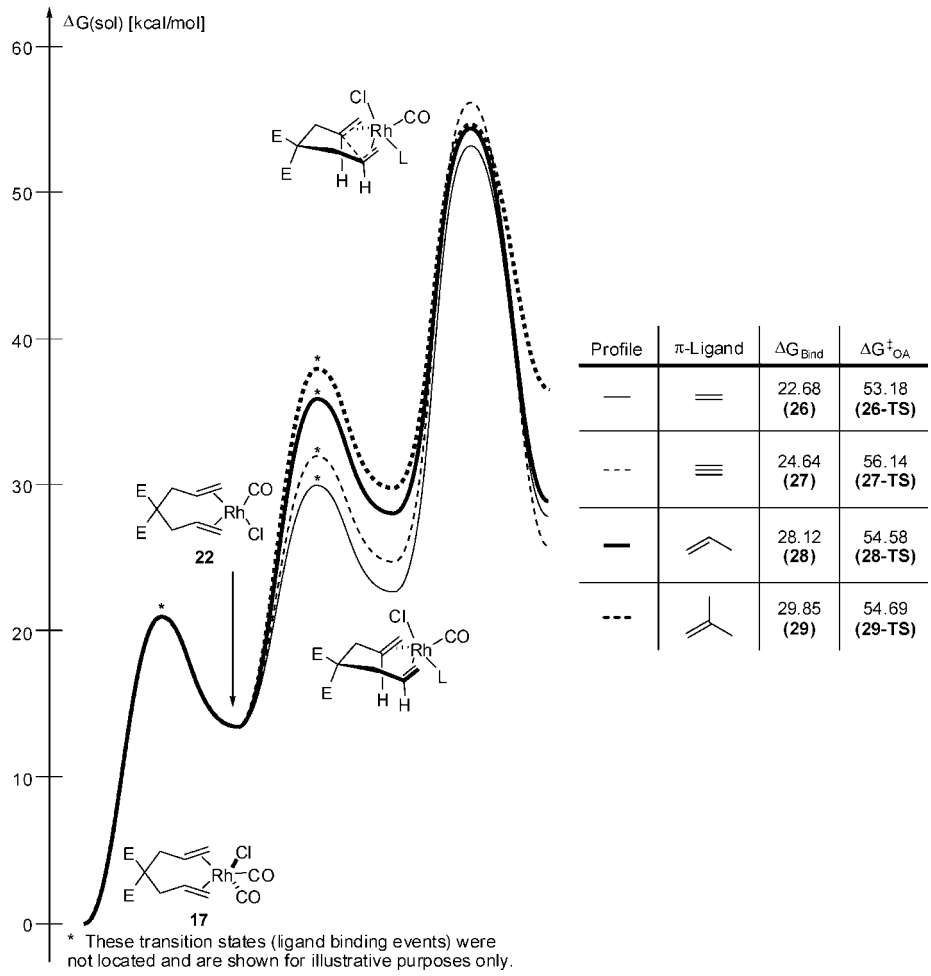

Figure 14. Binding and activation energies for π-donors in the bis-ene system.

oxidative addition transition state **17-TS** is prohibitively high in energy, giving a barrier of 36.7 kcal/mol. As was the case with the diene-ene, the latter part of the catalytic cycle is reasonable, with the highest activation energy being that of the reductive elimination at 20.2 kcal/mol. This activation energy is low because the CO ligands continue to make the metal electron deficient, allowing for easy reduction.

We have considered that the metal fragment Rh(CO)Cl may act as the catalytically competent species (Figure 12). In the absence of the diene-fragment that can provide an additional π-ligand fragment to occupy the empty coordination after removal of the CO ligand, this mechanistic scenario gives rise to a four coordinate Rh(I) 16-electron complex **22** as the reactant complex. The computed reaction energy profile is shown in Figure 13. Not surprisingly, the oxidative addition transition state **22-TS** is extremely high in energy with a free energy of 43.5 kcal/mol. Thus, this reaction is unlikely to occur under any reasonable reaction conditions. The metal center in the five-coordinate 18-electron complex **17** is already electron deficient by virtue of the two CO ligands, and removing one of the CO ligands that function as σ-donors in addition to being π-withdrawing ligands results in an even more electron-deficient 16-electron complex that is unable to promote the oxidative addition reaction. In a similar arrangement as with the diene-ene Rh(CO)Cl case, the reductive elimination step is also prohibitively high, with an activation energy of 33.7 kcal/mol. Relative to **20-TS** in the $Rh(CO)_2Cl$ bis-ene catalytic cycle, **24-TS** is electron rich, which results in a destabilization of the transition state, leading to the high activation energy. In conclusion, our calculations provide a plausible explanation for why the carbocyclization of the bis-ene substrate is not possible. For the oxidative addition step to become kinetically feasible, one of the CO ligands has to be replaced by a less electron-withdrawing ligand, which was conveniently possible in the diene reactant by binding the diene fragment in η^4-fashion. With this conceptual picture at hand, it is easy to understand why reactant functionalizations shown in Scheme 1 failed to give the desired reaction. Most notably, our proposal suggests that the conceptually plausible π-conjugation does not play a significant role. Thus, replacing the vinyl moiety of **1** with a phenyl group in **4f** or any other noncoordinating π-components are not expected to facilitate the desired carbocyclization.

Our mechanistic analysis of the [2 + 2 + 1] carbocyclization of bis-ene substrates suggests a few rational design strategies. First of all, we may question whether or not the intramolecular π-base binding to afford the 18-electron complex **13** may be mimicked by an intermolecular π-base. Several π-base ligands were evaluated. The ligand binding energies and the activation energies for the oxidative addition are summarized in Table 2 and visualized in Figure 14. As predicted, the presence of the additional π-base makes the oxidative addition easier. For example, the energy difference between complex **29**, where isobutene is used as the additional π-base ligand, and the corresponding transition state **29-TS** is 24.8 kcal/mol, which is notably lower than the energy difference between **22** and **22-TS** that was computed to be 30.0 kcal/mol (Figure 13).

Scheme 4. Computed Energies of [2 + 2 + 1] Using $Rh(CO)_3^+$ as Catalyst (Energies Are Given in kcal/mol)

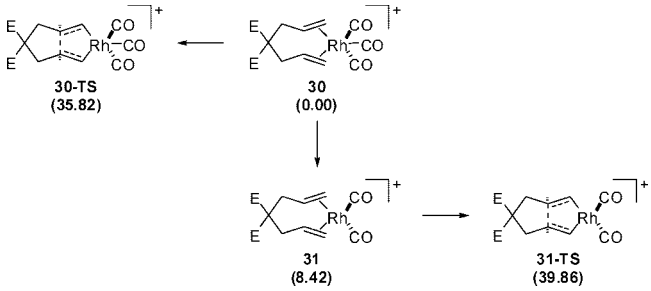

However, the binding of the π-ligand is in all cases energetically uphill, unfortunately. In the case of isobutene, the intermolecular ligand exchange of CO with the π-base ligand requires a free energy penalty of 29.9 kcal/mol, resulting in an overall activation barrier of 54.7 kcal/mol relative to the initial reactant complex **17**. The energy components enumerated in Table 2 reveal that the entropic advantage of releasing CO, observed for the intramolecular process **7** → **13** (Table 1) is lost. Whereas the release of CO, **17** → **22**, is again preferred entropically by 10.8 kcal/mol, essentially the same amount of energy, 11.2 kcal/mol, is lost when the free π-base is coordinated in the reaction **22** → **26**. Similar trends can be observed for all four π-bases tested in this work (Table 2). This observation highlights the reason why tethering the π-base to the bis-ene manifold, as is the case in the diene-ene substrate, is advantageous. By exchanging the CO ligand with an intramolecular π-component, the enthalpic benefit of ligand binding can be leveraged without having to pay the translational entropy penalty of a conventional intermolecular ligand exchange. This insight also suggests that there is nothing "magical" about the diene unit — tethering π-bases in a fashion that will allow for a sterically relaxed binding should in principle facilitate the oxidative addition in general. We are currently exploring this strategy, considering a number of different linkers. Another interesting observation illustrated in Figure 14 is that increasing the electron-donating abilities of the π-base ligands has little influence on the activation barrier, as all of the transition states located fall in a narrow range of energies. Thus, changing the electronics of the π-base is not a promising avenue for reaction design.

A second plausible strategy to be considered for controlling the reaction is the removal of the chloride ligand. Experimentally, the addition of silver salts is often observed to be beneficial in carbocyclization reactions involving metal chlorides. Presumably, the silver salts remove halides from the metal center, giving access to $Rh(CO)_x$ fragments. Removing halogen ligands that are σ-electron withdrawing is a plausible strategy for increasing the electron density at the metal center to facilitate oxidative addition. We modeled this scenario by using $Rh(CO)_3^+$ as the catalytically active fragment to give the reactant complex **30** (Scheme 4). For the oxidative addition of **30**, we were able to locate the transition state **30-TS** with a solution-phase free energy of 35.8 kcal/mol, which is very comparable to 36.7 kcal/mol obtained for **17-TS**. Loss of CO to form **31** is still endergonic, albeit 5.1 kcal/mol lower in energy than **22**. The oxidative addition traversing **31-TS** is still prohibitively high, but at 39.9 kcal/mol, it is 3.7 kcal/mol lower in energy than **22-TS**. Thus, we conclude that the removal of the chloride ligand does not influence the overall energetics of the reaction notably.

The final functionalization strategy that we considered relates to the nature of the halogen ligand. Whereas the removal of the halogen ligand and subsequent addition of a CO ligand does not give rise to the desired lowering of the transition-state energy, as discussed above, we questioned how sensitive the transition-state energy is to ligand exchange at this position in general. The simplest test case is of course to exchange the chloride ligand by the less electronegative bromide group. The complete catalytic cycle using $Rh(CO)_2Br$ as the active fragment is shown in Figure 15. The barrier for the oxidative addition associated with the transition state **32-TS**, 31.3 kcal/mol, is significantly lower than in the chloride analogue where the barrier was computed to be 36.7 kcal/mol. However, 31.3 kcal/mol is still too high to be feasible under mild reaction conditions. In accord with the diene-ene and $Rh(CO)_2Cl$ mediated bis-ene [2 + 2 + 1] reaction, the reductive elimination (**35-TS**) is possible, with an activation energy of 21.9 kcal/mol. Interestingly, the analogous iodide complex shows practically identical energies and structures (see Supporting Information for details). For completeness, we have also simulated the reaction energy profile using the Rh(CO)Br fragment as the catalytically active component, and its energy profile is shown in Figure 16. While the oxidative addition via **37-TS** has been lowered by 4.6 kcal/mol compared to **22-TS**, the decreased electronegativity of bromine was not enough to bring the energy requirements of this catalytic cycle into a more useful range. As before, a continuing trend in the use of Rh(CO)Br is that the reductive elimination (**39-TS**) is also energetically unfavorable with a barrier of 34.6 kcal/mol.

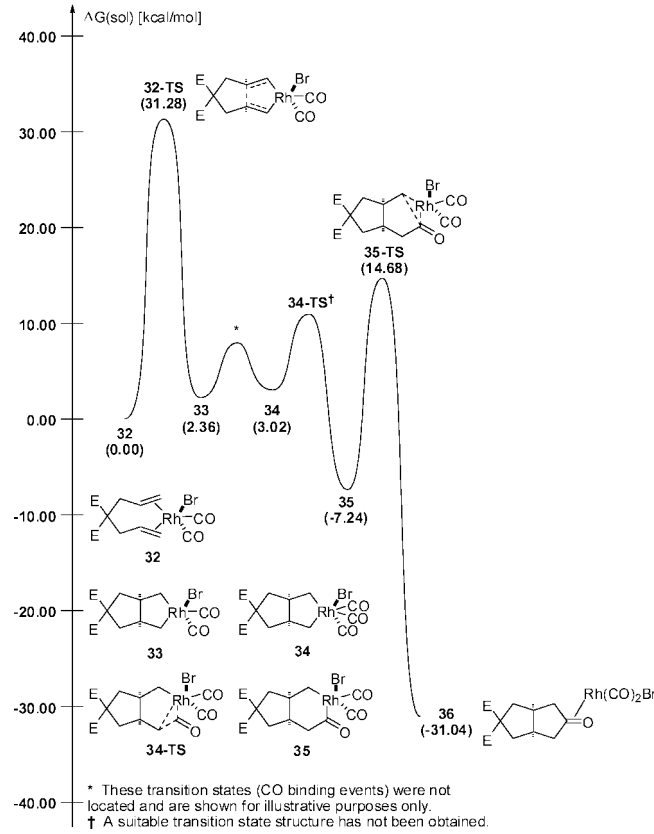

Figure 15. Reaction energy profile for bis-ene [2 + 2 + 1] using $Rh(CO)_2Br$.

Conclusions

In conclusion, we have constructed a complete reaction energy profile for the rhodium(I)-catalyzed [2 + 2 + 1] Pauson–Khand

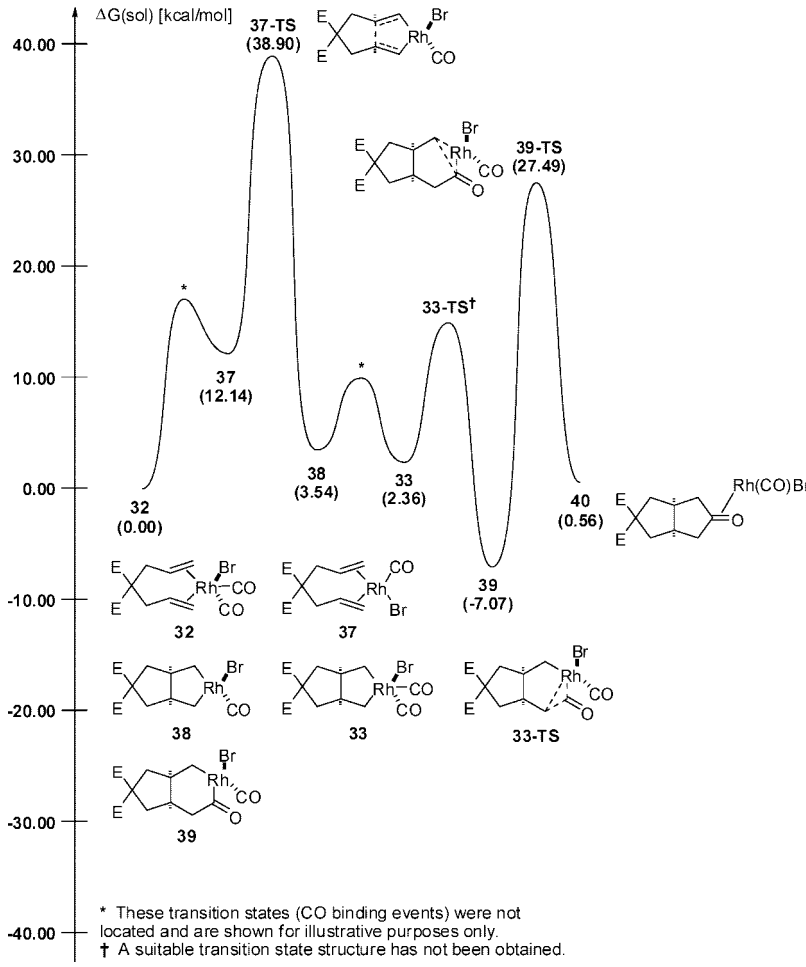

Figure 16. Reaction energy profile for bis-ene [2 + 2 + 1] using Rh(CO)Br.

carbocyclization, delineating the relationship between the functional groups of the reaction and the catalyst composition. We found that the addition and removal of CO to control the electron density at the metal center is crucial to facilitating the two most demanding steps of the catalysis, the oxidative addition to form the metallacycle and the reductive elimination to liberate the final product. Diene-ene substrates make excellent carbocyclization candidates due to the presence of the additional π-base fragment in the diene moiety, which allows the metal to be coordinatively saturated during the critical oxidative addition step, after releasing a CO ligand. Bis-enes, on the other hand, lack viable π-base fragments that can undergo rearrangement to facilitate CO loss. We have explored a few plausible functionalization strategies, and while we were thus far unable to identify a reactant−catalyst combination that may afford a successful carbocyclization of simple bis-enes, as seen for the diene-ene reactant, we have demonstrated and classified the conceptually plausible strategies in both qualitative and quantitative sense. This work forms the foundation for further explorations of the Pauson−Khand reactions. Our study demonstrates clearly that the increase of scope and functional group tolerance is likely to require a more complicated Rh-catalyst that gives a higher degree of structural design.

Acknowledgment. We thank the NSF (0116050 and CHE-0645381) for financial support. M.H.B. is a Cottrell Scholar of the Research Corporation and an Alfred P. Sloan Fellow of the Alfred P. Sloan Foundation. W.H.P. and R.L.L. thank the Department of Education for financial support through GAANN fellowships and R.L.L. thanks the Merck Research Corporation for a graduate fellowship.

Supporting Information Available: Cartesian coordinates of computed structures, energies, vibrational frequencies, and additional discussion. This material is available free of charge via the Internet at http://pubs.acs.org.

JA800856P